Contribution from the Max-Planck-Institut für Festkörperforschung, 7000 Stuttgart 80, Federal Republic of Germany

Metal–Metal Bonding in Transition-Element and Lanthanoid Cluster Halides

D. W. BULLETT*

Received November 2, 1979

Metal–metal bonding in transition-element and lanthanoid cluster halides is discussed with use of the results of electron density of states calculations for NbI_4, Nb_3I_8, ZrCl, ScCl, GdCl, and Gd_2Cl_3. NbI_4 is shown to be a semiconductor with an energy gap ~0.4 eV separating the filled metal–metal pair bonds from higher d bands; the ionic charge configuration is approximately $Nb^{2.0+}(I^{0.5-})_4$. In a single layer of Nb_3I_8, six electrons provide three low-lying metal–metal bonds while the uppermost electron sits unpaired in a localized state; neighboring Nb_3 clusters are too widely separated to allow delocalization and metallic conductivity. The Fermi level in ZrCl lies in a deep minimum in the density of states, but there is a slight metallic overlap between the three occupied metal–metal bonding bands and the higher d bands. Charge transfers from metal to halogen are approximately 0.5 e for ZrCl and 0.8 e for ScCl and GdCl. A semiconducting band gap of ~0.7 eV is predicted for Gd_2Cl_3.

Introduction

The synthesis and characterization of binary compounds of low-valent transition metals[1–5] and rare earths[5–8] have been a rapidly developing area over the last two decades. Important new discoveries have been made concerning the metal-rich halides of these elements (as well as the chalcogenides and pnictides[9] and the metal-rich oxides of alkali metals[10,11]). The structures and properties of these solids impose a severe strain on the conventional explanations of crystal packing, in terms of such concepts as the point-charge ionic model or the radius-ratio rules which govern the packing of hard spheres. In general, these compounds cannot be readily understood in terms of the usual valences of the constituent elements. Metal–metal bonding leads to the formation of discrete M_n clusters, with the number of metal–metal bonds increasing with the number of valence electrons on the metal atom. The concentration of valence electrons and the nonmetal to metal ratio (X/M) control the cluster size and the strength of bonding. Thus NbI_4 contains bonded pairs of metal atoms M_2,[12–14] Nb_3I_8 contains M_3 triangles[15] and $CsNb_4Cl_{11}$ contains planar M_4 rhombuses.[16] A very large number of binary structures may be described in terms of M_6X_8 or M_6X_{12} octahedral clusters, condensed to share corners, edges, or faces.[1–9] In the present investigation we look at the electronic structure of some of these systems, with a view to interpreting the bonding concepts involved. In particular, we have calculated the densities of electronic states in NbI_4 and Nb_3I_8 and in ZrCl, ScCl, GdCl, and Gd_2Cl_3.

Method of Calculation

The particular linear-combination-of-atomic-orbitals method used has already proved successful in accounting for the properties of transition-metal dichalcogenides,[17] trichalcogenides,[18] and chalcogenide halides.[19] The crystal potential is constructed from overlapping neutral-atom charge densities, with the exchange-correlation component approximated by the usual local-density form with proportionality constant $\alpha = 0.7$. Interactions between numerical atomic orbitals[20] are calculated in the two-center approximation. In a diatomic molecule AB free-atom orbitals would be postulated as solutions of a set of pseudo Schrödinger equations of the form[21]

$$H\phi_i - \phi_j \mathbf{S}_{jk}^{-1} \langle \phi_k | V' | \phi_i \rangle = \epsilon_i \phi_i \qquad (1)$$

Here the suffix i labels the atomic site and quantum numbers of the orbital which satisfies an isolated atom Hamiltonian, H_A or H_B. V' is the perturbation in the potential, caused by the presence of the second atom in the molecule. Thus in eq 1, V' is equal to $H - H_A$ for orbitals ϕ_i centered on atom A and is equal to $H - H_B$ for orbitals on atom B, where H is the one-electron Hamiltonian for the complete molecule AB. In the second term in eq 1, $\mathbf{S}^{-1}$ is the inverse of the overlap matrix of basis orbitals. The effect of this term is to project out most of the perturbation, thus justifying our use of undistorted atomic orbitals as approximate solutions of eq 1.[21]

Table I. Neutral-Atom Energy Levels Used in the Calculations (eV)

	Cl	I	Nb- ($d^{3.3}$)	Sc- (d^2)	Zr- (d^3)	Gd- (d^2)
s	−21.2	−16.5	−5.1	−4.9	−5.3	−4.3
p	−9.5	−7.7	−2.9	−2.8	−3.0	−2.6
d			−5.0	−2.7	−3.7	−2.9

In a more complicated structure we draw Wigner–Seitz spheres around each atom and calculate the matrix elements between orbitals on any pair of atomic sites by integration over the corresponding atomic spheres, ignoring contributions to the potential arising from the presence of other atoms. For a crystalline solid the basis functions can be chosen as Bloch functions Φ^k_i, and eq 1 takes the general form

$$H\Phi^k_i - \mathbf{D}^k_{ij}\Phi^k_j = \epsilon_i \Phi^k_i \qquad (2)$$

where i and j run over all atomic orbitals in the unit cell. With

* Correspondence should be addressed to the School of Physics, University of Bath, Bath BA2 7AY, England.

(1) H. Schäfer and H. G. von Schnering, *Angew. Chem.*, **76**, 833 (1964).
(2) F. A. Cotton, *Q. Rev., Chem. Soc.*, **20**, 389 (1966).
(3) M. C. Baird, *Prog. Inorg. Chem.*, **9**, 1 (1968).
(4) R. B. King, *Prog. Inorg. Chem.*, **15**, 287 (1972).
(5) A. Simon, *Chem. Unserer Zeit*, **10**, 1 (1976).
(6) J. E. Mee and J. D. Corbett, *Inorg. Chem.* **4**, 88 (1965).
(7) D. A. Lokken and J. D. Corbett, *Inorg. Chem.* **12**, 556 (1973).
(8) A. Simon, H. J. Mattausch, and N. Holzer, *Angew. Chem.*, **88**, 685 (1976); *Angew. Chem., Int. Ed. Engl.*, **15**, 624 (1976).
(9) H. F. Franzen, *Prog. Solid State Chem.* **12**, 1 (1978).
(10) A. Simon, *Z. Anorg. Allg. Chem.*, **395**, 301 (1973).
(11) A. Simon, *Struct. Bonding (Berlin)*, **36**, 81 (1979).
(12) J. D. Corbett and P. Seabaugh, *J. Inorg. Nucl. Chem.*, **6**, 207 (1958).
(13) L. F. Dahl and D. L. Wampler, *Acta Crystallogr.*, **15**, 903 (1962).
(14) L. F. Dahl and D. L. Wampler, *J. Am. Chem. Soc.*, **81**, 3150 (1962).
(15) A. Simon and H. G. von Schnering, *J. Less-Common Met.*, **11**, 31 (1966).
(16) A. Broll, A. Simon, H. G. von Schnering, and H. Schäfer, *Z. Anorg. Allg. Chem.*, **367**, 1 (1969).
(17) D. W. Bullett, *J. Phys. C*, **11**, 4501 (1978).
(18) D. W. Bullett, *J. Phys. C*, **12**, 277 (1979).
(19) D. W. Bullett, *J. Phys. C*, **13**, 1267 (1980).
(20) F. Herman and S. Skillman, "Atomic Structure Calculations", Prentice-Hall, New York, 1963.
(21) D. W. Bullett, *Solid State Phys.*, **35** (1980).

0020-1669/80/1319-1780$01.00/0

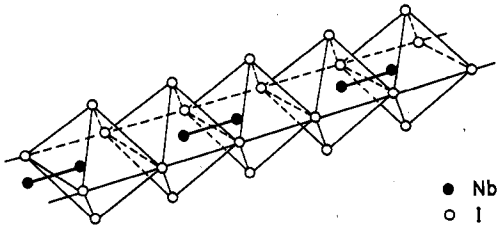

Figure 1. Schematic picture of the NbI_4 structure. NbI_6 octahedra share opposite edges in a linear chain. Nb atoms are displaced from the octahedron centers along the chain axis to form metal–metal bonds.

the assumption of linear independence of the basis orbitals, the energy eigenvalues and eigenfunctions, $\mathbf{E}^k_n$ and Ψ^k_n, of the crystal are given by diagonalizing the secular matrix $\mathbf{D}$

$$\det|\mathbf{D}^k - \mathbf{E}^k_n\mathbf{I}| = 0 \qquad (3)$$

In practice the two-center interactions decay quite rapidly with site separation. For convenience we set all interactions to zero for separations beyond 5 Å. The important shells of neighbors lie within this distance, and their interactions are included explicitly.

The basis functions used in the present work include s, p, and d valence-level orbitals on the transition-metal or lanthanoid atoms and s and p orbitals on the halogens. The neutral-atom energy levels for the appropriate atomic configuration are given in Table I. It is assumed that the 4f electrons on the rare-earth atoms are sufficiently localized that these orbitals can be entirely left out of the calculation, so that these rare earths behave just like trivalent transition elements. The use of neutral-atom energy levels and charge densities is of course a fairly severe approximation but a necessary one to retain computational simplicity for the more complex structures. The most vulnerable feature of this approximation is likely to be the relative positions in energy of the iodine valence bands compared to the metal d bands, where errors of order 1 eV might be expected; less sensitive are the individual features of the separate d subbands which are our main concern in studies of metal–metal bonding.

Quite large ionicities are suggested by some of the results, and it may be argued that these are inconsistent with the use of neutral-atom energy levels, but the problem is partly one of semantics. Most of the transferred charge is contributed by transition-element s electrons rather than d electrons, and the diffuse nature of the s orbitals means that it makes little difference to the potential if we attribute this charge to the surrounding ligands.

NbI_4. Several niobium iodides have been synthesized and characterized by Corbett and Seabaugh[12] including two different forms of niobium tetraiodide. We deal here with only the low-temperature ($T < 348$ °C) form, α-NbI_4, the structure of which has been determined by Dahl and Wampler.[13] The crystals are orthorhombic, space group $Cmc2_1$, with eight formula units per cell.

The most important aspect of the structure for present purposes is that it contains infinite chains parallel to the a axis of NbI_6 octahedra sharing opposite edges (Figure 1). Niobium atoms are displaced 0.26 Å from the center of the iodine octahedra to give alternate short (3.3 Å) and long (4.3 Å) Nb–Nb distances (cf. 2.86 Å in niobium metal). Iodine atoms are arranged in the unit cell in an approximately, hexagonal close-packed array, with niobium atoms occupying one-fourth of the available octahedral interstices to form the linear chains by filling alternate rows of octahedral holes in alternate layers.

Figure 2 displays the calculated density of electron states in the highest valence and lowest conduction bands, both for the full three-dimensional unit cell and for an isolated chain taken from the structure. The former histogram was calculated by diagonalizing the (100 × 100) secular matrix at a

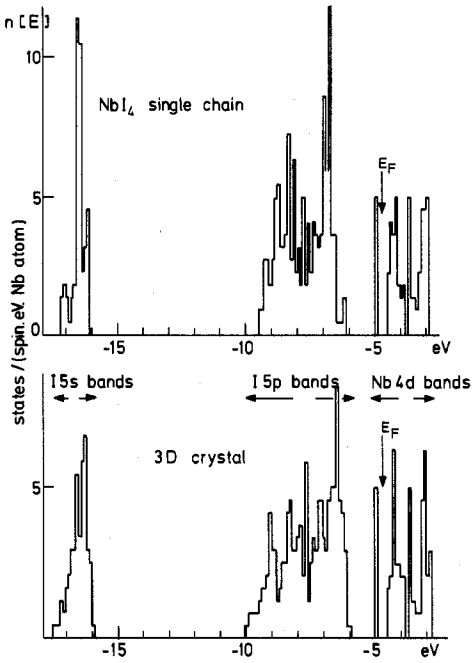

Figure 2. Density of valence and conduction states in NbI_4, calculated for an isolated chain and for the full three-dimensional crystal. The Fermi level E_F lies in the gap which separates metal–metal bonding states at −4.9 eV from higher Nb d states.

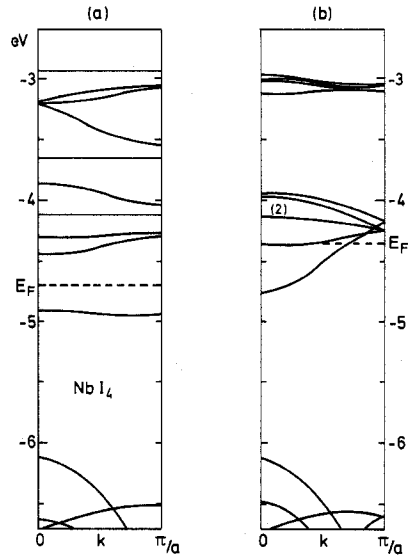

Figure 3. One-dimensional energy bands near the Fermi level in NbI_4: (a) observed single chain of NbI_4; (b) a chain containing no Nb–Nb pairing along the chain axis.

sample of six $\mathbf{k}$ points in the irreducible Brillouin zone and the latter by diagonalizing the (50 × 50) matrix at twelve $\mathbf{k}$ points in the one-dimensional zone. The results are essentially the same in either case. Iodine 5s orbitals form a band of states centered at −16.6 eV and of width ~1.2 eV. The broader valence band centered at −8 eV is composed predominantly of iodine p orbitals. This band is 3.6 eV wide for the single chain and broadens slightly to 4.1 eV when interchain interactions are included; at the same time the sharp one-dimensional band-edge singularities are partially smoothed as expected in the three-dimensional crystal. There then follow, in order of increasing energy, a group of very narrow bands which are essentially the transition-element d bands. Since the interchain Nb–Nb distance is large (~7 Å), there is very little difference between the bands calculated for a single chain or for coupled chains. One d band is split off at a distinctly

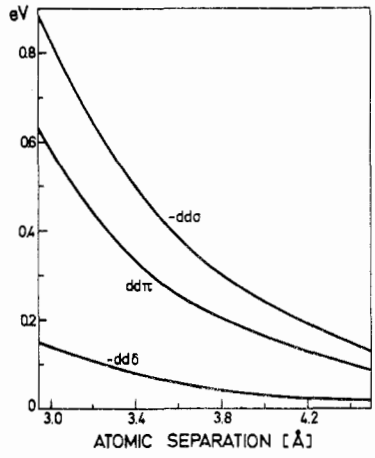

Figure 4. Rate of decay of the two-center interatomic matrix elements $dd\sigma$, $dd\pi$ and $dd\delta$ as a function of the separation between Nb atoms.

higher binding energy than the others and forms the highest occupied band. The calculated energy gaps between the highest occupied and lowest unoccupied states are 0.41 eV for the single chain and 0.38 eV for the full three-dimensional structure.

Figure 3 shows details of the one-dimensional energy bands in the vicinity of the Fermi level. It is easy to see how the doubling of the unit-cell length via pairing of Nb atoms establishes a filled band of metal–metal bonds (comprised essentially of d_{z^2} orbitals pointing toward the neighboring metal atom) below the other empty d bands. In Figure 3b we see the d bands, without such a distortion, for an idealized chain in which Nb atoms sit exactly at the centers of the coordinating iodine octahedra. The d states split in the octahedral field into the familiar triplet and doublet, separated by $\sim$1.2 eV. Within the triplet, the d_{z^2} orbitals pointing along the chain axis form the broadest band, extending from −4.8 to −3.9 eV. This width is readily understood from the rate of decay of the two-center $dd\sigma$ interaction as a function of the Nb–Nb separation (Figure 4). For a separation of $a/2 = 3.83$ Å, $dd\sigma$ is equal to −0.28 eV and a purely d_{z^2} band in the regular one-dimensional chain would have a width of $4dd\sigma = 1.1$ eV. Hybridization with the iodine p orbitals and Nb s and p orbitals reduces this slightly. In the distorted chain Nb–Nb separations are alternately 3.3 and 4.3 Å, and the d_{z^2} band splits into bonding and antibonding subbands. The relevant $dd\sigma$ interactions are then −0.56 and −0.16 eV; thus purely d_{z^2} subbands should extend in the ranges $E_d - 0.56 \pm 0.16$ eV and $E_d + 0.56 \pm 0.16$ eV. Complicated rehybridization effects take place in the distorted octahedral field, but we can identify the lower subband with that at −5.0 eV in Figure 3a. Complete occupation of this bonding band stabilizes the structure by lowering the average energy of the filled d states. An analogous Peierls distortion to a metal–metal-paired state is responsible for the different structures of $ZrSe_3$ and NbS_3.[18,22]

The electrical properties of NbI_4 have been studied by several workers. Kepert and Marshall[23] reported an activation energy for conduction of 0.12 eV at atmospheric pressure. For a Fermi level in midgap, this would suggest a semiconducting gap $\sim$0.24 eV, slightly smaller than the value calculated here. High-pressure measurements[24,25] show that the resistivity decreases monotonically with pressure. The activation energy

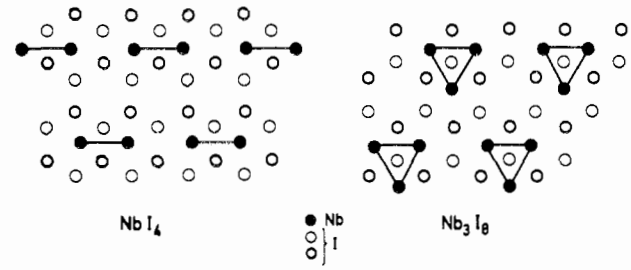

Figure 5. Nb_2 pairs and Nb_3 triangles in the crystal structures of NbI_4 and Nb_3I_8. Light and bold open circles denote the hexagonal array of I atoms above and below the plane of the metal clusters. Intra- and intercluster Nb–Nb distances are 3.3 and 4.3 Å in NbI_4 and 3.0 and 4.6 Å in Nb_3I_8.

decreases to 0.06 eV at 100 kbar and to 0.02 eV at 130 kbar. At about 150 kbar the temperature coefficient of resistivity becomes positive, and NbI_4 shows metallic behavior with a typical linear temperature dependence of resistivity. Presumably under increasing pressure the separate chains are forced together, broadening the iodine valence bands and thus tending to push up the Nb bonding band. At the same time the compression of iodine–iodine distances within a chain forces the Nb atoms back toward the centers of the octahedra. Eventually the difference between successive Nb–Nb separations becomes so small that indirect band overlap occurs between the lowest metal–metal bonding band and the next higher d band.

Related crystal structures are found for niobium tetrabromide[1,26] and tetrachloride.[1,27] The smaller the size of the anion, the greater is the distortion in the ratio of Nb–Nb distances as the paired atoms may come closer together and bond more strongly. These stronger metal–metal bonds are reflected in the higher activation energies for conduction in $NbCl_4$ and $NbBr_4$ compared to NbI_4: 0.44, 0.37, and 0.12 eV, respectively.[23]

A useful, elementary way to assign the charge in an LCAO wave function to the various atomic sites involves dividing all overlap charges equally between the corresponding atoms.[17] We can then assess the ionicity by filling the appropriate number of levels in the local atomic densities of states. From such a procedure it is found that approximately 0.5 electron is transferred from the Nb atom to each iodine atom, $Nb^{2.0+}(I^{0.5-})_4$.

Nb_3I_8. Like NbI_4, the crystal structure of Nb_3I_8[15] is based on the occupation by niobium atoms of octahedral interstices in a hexagonal close-packed array of iodine atoms (Figure 5). Niobium atoms occur in alternate layers, and one-fourth of the sites are left empty within each occupied layer. The result is a two-dimensional layer structure closely related to CdI_2. The Nb atoms are displaced from the centers of iodine octahedra to form triangular clusters of metal atoms. Nb–Nb distances within a cluster are 3.0 Å, compared to the shortest Nb–Nb distances of 4.6 Å between clusters.

The densities of states calculated for the true two-dimensional structure and for an idealized structure with metal atoms in perfect octahedral positions (i.e., without metal–metal bonding) are displayed in Figure 6. Only the iodine p and metal d bands are shown; the iodine 5s orbitals were also included in the basis and form bands of similar energy position and width to those of NbI_4. The octahedral ligand field splitting of the Nb d states is again clear in Figure 6a, with a band of three states per metal atom extending from −5.0 to

(22) D. W. Bullett, *J. Solid State Chem.*, in press.
(23) D. L. Kepert and R. E. Marshall, *J. Less-Common Met.*, **34**, 153 (1974).
(24) H. Kawamura, I. Shirotani, and K. Tachikawa, *Phys. Lett. A*, **65**, 335 (1978).
(25) H. Kawamura, I. Shirotani, and K. Tachikawa, *J. Solid State Chem.*, **27**, 223 (1979).
(26) H. Schäfer and K.-D. Dohmann, *Z. Anorg. Allg. Chem.*, **311**, 134 (1961).
(27) H. G. von Schnering and H. Wöhrle, *Angew. Chem. Int., Ed. Engl.*, **2**, 558 (1963).

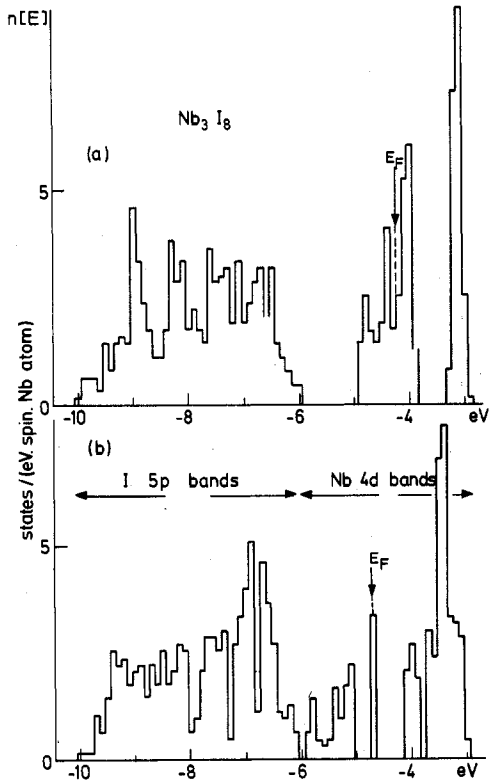

Figure 6. Valence and conduction band densities of states calculated for Nb_3I_8. The upper histogram is for a hypothetical structure in which Nb atoms sit exactly at the centers of the coordinating iodine octahedra; the lower histogram is for the real structure containing metal–metal bonds.

−3.9 eV and a narrower band containing two states per metal atom between −3.4 and −2.9 eV. The broad valence band from −10 to −6 eV, which we may formally describe as the iodine p band, can contain 8 of the 15 electrons per formula unit coming from the metal electrons. The distortion into triangular clusters moves three metal d bands strongly down to energies between −6 and −5.1 eV in Figure 6b. These we can clearly label as the metal–metal bonds between the three pairs of atoms in Nb_3 triangles. The fourth d band is separated by 0.5 eV from higher d bands and is half-filled in undoped Nb_3I_8. However, the calculated bandwidth of this state is extremely narrow (0.04 eV), and the assumption that these states are delocalized cannot be justified; each state will be localized within a particular Nb_3 triangle. An activation energy of 0.26 eV has been measured for conduction in the *ab* plane of Nb_3I_8.[25]

Zr, Sc, and Gd Monochlorides. The structures of the metal-rich monohalides are of the hexagonal-layer type in which close-packed double layers of metal M atoms alternate with widely spaced double layers of nonmetal X atoms (XMMX..XMMX). These are closely related to the Ag_2F,[28] Hf_2S[29] (MMXMMX), and CdI_2 (XMX..XMX) structures. For ZrCl[30–32] and GdCl[8] and similarly TbCl[8] the stacking sequence is abca..bcab..cabc while for ScCl[33] (which is isostructural with ZrBr[34] and HfCl[34,35]) the sequence is abca..

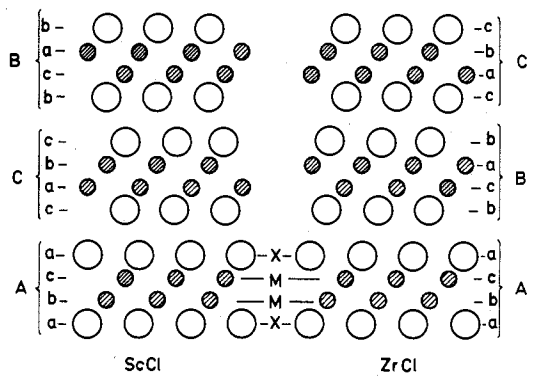

Figure 7. Stacking sequences of halogen (X) and metal (M) close-packed layers in the ScCl and ZrCl structures. The individual sandwiches (labeled A, B, and C) are the same in both structures.

Table II. Some Interatomic Distances in ScCl, ZrCl, and GdCl (A)

	no. of neighbors	ScCl	ZrCl	GdCl
M–M interlayer	3	3.22	3.09	3.55
intralayer (a)	6	3.47	3.42	3.82
M–Cl	3	2.59	2.63	2.82
Cl–Cl intralayer (a)	6	3.47	3.42	3.82
intersandwich	3	3.70	3.61	3.61

cabc..bcab; the different types of packing correspond to different sequences of similar four-layer XMMX sandwiches (Figure 7).

Both structures[32–34] belong to the trigonal $R\bar{3}m$ space group and have a 12-layer repeat distance in the *c* direction (corresponding to 3 XMMX sandwiches). The lattice constant within the layer is just the intralayer nearest-neighbor distance. Using lower case letters a, b, and c to denote the relative displacement of layers perpendicular to the *c* axis and capital letters to denote the X atom positions in identical four-layer XMMX sandwiches, we can describe the unit cell sequence as ABC in ZrCl and ACB in ScCl. Both structures present identical trigonal antiprismatic coordination of metal atoms with respect to the three M and three X neighbors in adjoining layers of the same sandwich. The difference lies in the coordination of the X atoms by M (same sandwich) and X (adjacent sandwich) in adjoining layers; this is trigonal prismatic for ScCl but antiprismatic for ZrCl.

A very enlightening view of the sandwich structure and its reduction from other structures such as Gd_2Cl_3[7] and Sc_7Cl_{10}[37] comes from considering MX as a condensed two-dimensional array of edge-sharing M_6X_8 clusters.[8,36]

These metal-rich monochlorides show physical properties consistent with strong metal–metal bonding within the sandwich and weak van der Waals like interactions between sandwiches. Thus they form graphite-like platelets with easy cleavage normal to the *c* axis but display high thermal stabilities and high melting points.[8,32–34] The small size of available crystals and their reactivity and laminar nature make direct measurements of their highly anisotropic electrical conductivity difficult, but photoelectron spectra for both ZrCl and ZrBr have established unambiguously their metallic character in terms of a nonzero density of states at the Fermi level E_F.[34]

Some of the typical coordination distances are shown in Table II. Since intersandwich distances are relatively large,

(28) G. Argay and I. Náray-Szabó, *Acta Chim. Acad. Sci. Hung.*, **49**, 329 (1966).
(29) H. F. Franzen and J. Graham, *Z. Kristallogr., Kristallgeom., Kristallphys., Kristallchem.*, **123**, 133 (1966).
(30) S. I. Troyanov, *Vestm. Mosk. Univ., Khim.*, **28**, 369 (1973).
(31) S. I. Troyanov and V. I. Tsirel'nikov, *Russ. J. Inorg. Chem.* (*Engl. Transl.*), **15**, 1762 (1970).
(32) D. G. Adolphson and J. D. Corbett, *Inorg. Chem.*, **15**, 1820 (1976).
(33) K. R. Poppelmeier and J. D. Corbett, *Inorg. Chem.*, **16**, 294 (1977).
(34) R. L. Daake and J. D. Corbett, *Inorg. Chem.*, **16**, 2029 (1977).
(35) A. S. Izmailovich, S. I. Troyanov, and V. I. Tsirel'nikov, *Russ. J. Inorg. Chem.* (*Engl. Transl.*), **19**, 1597 (1974).
(36) A. Simon, N. Holzer, and H. J. Mattausch, *Z. Anorg. Allg. Chem.*, **456**, 207 (1979).
(37) K. R. Poppelmeier and J. D. Corbett, *Inorg. Chem.* **16**, 1107 (1977).

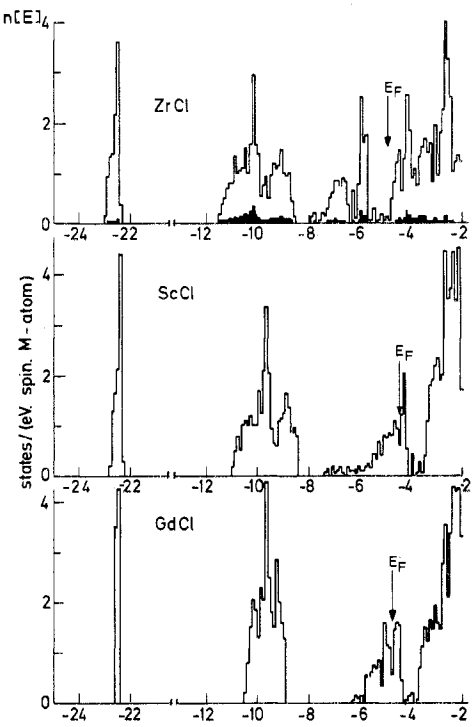

Figure 8. Single-sandwich densities of valence-band and conduction-band states for ZrCl, ScCl, and GdCl. The shaded regions in the histogram for ZrCl represent the transition-metal contribution to states in the Cl s and p bands and the Cl contribution to states in the Zr 4d band.

we consider here only the electronic structure of a single four-layer sandwich in order to greatly reduce the size of the secular matrix. Furthermore, the metal atoms constitute the filling inside the sandwich and metal–metal bonding should not be sensitively influenced by interlayer halogen interactions (although it has been observed that the cohesive forces between sandwiches are considerably stronger in ZrBr and ScCl than in ZrCl[33,34]). Discussions of the possible causes behind the different stacking sequences of sandwiches have been given elsewhere.[33,34]

The calculated electron densities of states for the single sandwiches are shown in Figure 8. Each was calculated from a grid of ten regularly spaced **k** points in the irreducible Brillouin zone. The unit cell contains two MX formula units to give a secular matrix of order (26 × 26).

In each case the Cl 3s and 3p states are prominent in bands centered at −22.5 and −10 eV, respectively. The decreasing width of the bands as we proceed from ZrCl to ScCl to GdCl reflects the increasing intralayer lattice constant a and the higher d level in Sc compared to Zr. Atomic Gd 4f orbitals have been omitted from the band structure calculation, but from the initial atomic calculation for a neutral $4f^7$ configuration they should form localized levels at about −12.2 eV.

States between −8 and −2.5 eV are essentially composed of transition-metal or lanthanoid d orbitals. The presence of strong covalent-like metal–metal bonding is particularly evident in ZrCl, where the Fermi level E_F falls at −4.5 eV in a deep (but nonzero) trough in the density of states $n(E)$. The local coordination of Cl and M atoms about each metal atom is such as to drive substantially down in energy three of the ten d bands per unit cell. We can tentatively identify the double occupation of these three bands with the establishment of strong bonds between each Zr atom and its nearest-neighbor Zr atoms in the adjacent layer.

The similarity of the scandium and rare-earth monochloride crystal structures to the ZrCl structure is at first sight surprising, as these have formally only two rather than three

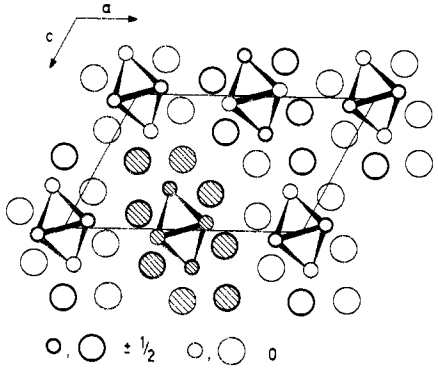

Figure 9. The Gd_2Cl_3 structure[36] projected on a plane normal to the chain direction. The shaded atoms were used in a linear representation of the crystal; this one-dimensional cell contains the four Cl atoms capping triangular faces of the Gd octahedra, together with four bridging Cl atoms normally shared between two chains.

electrons per metal atom available for metal–metal bonding. We might perhaps have expected a symmetry-lowering distortion in which each metal atom would become more strongly bonded to two of its interlayer neighbors at the expense of the third. In fact, even in the trigonal environment the Fermi level for the reduced number of electrons falls below the sharp maximum in this energy region of $n(E)$, and the ZrCl-type sandwich is still stable for these trivalent metal chlorides. As a consequence of the smaller number of metal–metal bonding electrons, the difference between interlayer and intralayer M–M separations is less marked than for ZrCl, and the trough in $n(E)$ at about −5 eV for ScCl and GdCl is about 0.2 eV narrower than for ZrCl.

The main features of the calculated density of states for ZrCl are quite consistent with the X-ray photoelectron spectra measured by Daake and Corbett[34] for the valence region of ZrCl. The experimental spectrum shows Cl 3s and 3p and Zr 4d peaks centered 17.3, 6.4, and 1.2 eV, respectively, below the Fermi level. The calculated Cl p band lies about 1 eV too high in energy. Photoemission peak widths at half-maximum are approximately 2.7 eV for the p band and 2.1 eV for the d band.

It is also of interest to assess the extent to which valence and conduction bands are truly "p bands" and "d bands". A procedure for sharing the charge in each wave function between the different atomic sites was introduced in the discussion of NbI_4. The local atomic components of the density of states resulting from such an assignment are shown for ZrCl in Figure 8. It is clear that states near E_F really are predominantly d states and that the charge transferred to the halogen is considerably less than a full electron. The charge states obtained by pouring in the requisite number of electrons in this case are $Zr^{0.5+}Cl^{0.5-}$ and for the other two monohalides considered are $Sc^{0.8+}Cl^{0.8-}$ and $Gd^{0.8+}Cl^{0.8-}$.

Gd_2Cl_3. Gd_2Cl_3 crystallizes in an unusual structure[7] containing infinite linear chains of metal octahedra which share opposite edges and are elongated in the chain direction. Chlorine atoms are located off triangular faces of the octahedra and as bridges between the chains of octahedra. The structure may be viewed[8,36] as a linear condensation of M_6X_8 octahedral clusters into single chains, analogous to the double chains of edge-sharing M_6X_8 clusters in Sc_7Cl_{10},[37] the layers of edge-sharing M_6X_8 clusters in ScCl[33] and GdCl,[8] and the single chains of trans-edge-sharing M_6X_{12} clusters in Sc_5Cl_8.[38]

The complete structure contains two chains, or four formula units, per unit cell, and the (120 × 120) matrix dimension for

(38) K. R. Poppelmeier and J. D. Corbett, *J. Am. Chem. Soc.*, **100**, 5039 (1978).

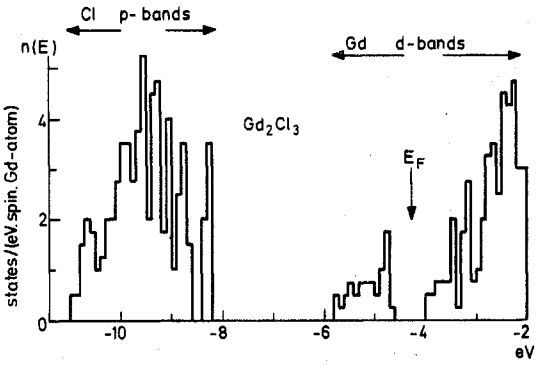

Figure 10. Calculated density of states for a single chain taken from the Gd_2Cl_3 structure. Metal–metal bonding states between −5.8 and −4.6 eV are separated from higher d bands by a 0.7 eV semiconducting gap.

a full band structure calculation would be inconveniently large. Instead we concentrate on the one-dimensional electronic structure of a single chain, $[(Gd_4Cl_8)^{2-}]_n$. This contains the backbone of metal octahedra from one of the chains in the unit cell and the chlorine atoms capping triangular side faces of the octahedra, together with the four bridging chloride ions which are shared between two chains in the full structure (Figure 9). Our single chain preserves the local environment of each metal atom in the real crystal.

The resulting density of states in the Cl p bands and Gd d bands shows the interesting form in Figure 10. The three lowest d bands hybridize to much lower energies than the remaining seventeen, and it is the double occupation of these three low-lying bands that stabilizes the structure. A gap of 0.7 eV separates the highest occupied and lowest unoccupied states of the single chain, and we might therefore expect to find a semiconducting gap which is only slightly smaller in the real crystal. The measurement of the conductivity along the axis of a one-dimensional metal is of course notoriously difficult, but certainly no metallic conduction has been observed in Gd_2Cl_3.[6,7] Very recent experimental evidence from photoemission and from temperature-dependent conductivity studies provide further support that Gd_2Cl_3 is a semiconductor.[39]

No simple covalent bond picture of the three lowest bands appears to be possible in this case. Only one Gd–Gd approach (the 3.35-Å edge shared by adjoining octahedra) per formula unit is perceptibly shorter than the others (~3.8 Å), and the upper two filled bonding states per octahedron are complicated hybrids which cannot be assigned simply to atom pairs.

Conclusion

We conclude that an LCAO calculation of the one-electron band structure can give a good quantitative account of metal–metal bonding in transition-element and rare-earth condensed-cluster halides. For each of the compounds considered the Fermi level lies at or near a deep minimum in the density of states, separating metal–metal bonding states from higher d states. It is the occupation of the metal–metal bands that stabilizes the rather unusual crystal structures formed by some of these compounds, especially Gd_2Cl_3, where the linear chain of edge-sharing distorted Gd octahedra provides a semiconducting gap of 0.7 eV in what one might have expected[7] to be a d band continuum.

Registry No. NbI_4, 13870-21-8; Nb_3I_8, 12030-01-2; ZrCl, 14989-34-5; ScCl, 17775-46-1; GdCl, 40603-48-3; Gd_2Cl_3, 12506-69-3.

(39) W. Bauhofer and G. Ebbinghaus, private communication.

Contribution from the Department of Chemistry, Università della Calabria, 87030 Arcavacata (CS), Italy

Metal Catecholato Complexes: A Source for Metallo-Labeling Antigens

OTTAVIO GANDOLFI,* GIULIANO DOLCETTI,* MAURO GHEDINI, and MICHAEL CAIS

Received August 6, 1979

New Pd(II) and Pt(II) carboxyl- and amine-substituted catecholato complexes of the type $L_2M(1,2\text{-}O_2C_6H_3\text{-}4\text{-}R)$ (L = $^1/_2$ bpy, M = Pt, R = CO_2H; L = $^1/_2$ COD, M = Pt, R = CO_2H or $CH_2CH_2CO_2H$; L = PPh_3, M = Pd or Pt, R = $CH_2CH_2NH_2$) have been prepared and characterized by elemental analysis and IR and NMR spectra. The possibility of forming a covalent bond with organic molecules through the free organic function of metal catecholates, for metallo-immunoassay (MIA) application, has been tested by preparing several amide derivatives. Thus bis(phosphine)palladium(II) and -platinum(II) carboxyl-substituted catecholates have been converted to their respective active esters and subsequently reacted with amines. Amide derivatives were obtained also with the new palladium(II) and platinum(II) amine-substituted catecholates, by reaction with phenylacetic active esters. All the isolated products were characterized by elemental analysis and IR and NMR spectra. A different chemical behavior has been found in the case of the bis(phosphine)palladium(II) catecholato complexes, in which displacement of phosphine occurred in the presence of amines.

Introduction

In the last decade there has been a continuous expansion in the work of metal complexes associated to biological derivatives for medical, pharmacological, and biological applications.

Moreover, a recent nonisotopic system, designated as metalloimmunoassay (MIA),[1] had opened an interesting new dimension for the use of transition-metal atoms in their form of organometallic compounds. The feasibility of MIA has been demonstrated,[2] and its principle is based on the replacement of radioisotopes with organometallic compounds as labeling agents for in vivo and in vitro immunological reactions. A necessary chemical requirement for MIA is the formation of stable "tailor-made" metallo antigens. As already mentioned,[2] one approach for coupling transiton metals to organic mole-

* To whom correspondence should be addressed: O.G., Università della Calabria; G.D., Institute of Chemistry, University of Udine, 33100 Udine, Italy.

(1) M. Cais, S. Dani, Y. Eden, O. Gandolfi, M. Horn, E. E. Isaacs, Y. Josephy, Y. Saar, E. Solvin, and L. Snarsky, *Nature (London)*, **270**, 534 (1977).
(2) M. Cais, E. Slovin, and L. Snarsky, *J. Organomet. Chem.*, **160**, 223 (1978).

0020-1669/80/1319-1785$01.00/0